

# Probing Cell-Surface Carbohydrate Binding Proteins with Dual-Modal Glycan-Conjugated Nanoparticles

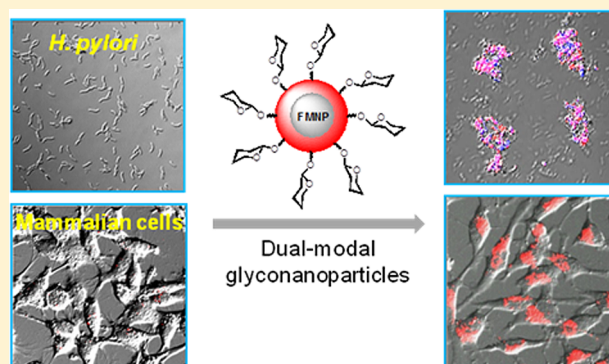
Sungjin Park,<sup>†,§</sup> Gun-Hee Kim,<sup>†,§</sup> Seong-Hyun Park,<sup>†</sup> Jaeyoung Pai,<sup>†</sup> Dominea Rathwell,<sup>†</sup> Jin-Yeon Park,<sup>‡</sup> Young-Sun Kang,<sup>‡</sup> and Injae Shin<sup>\*,†</sup>

<sup>†</sup>Department of Chemistry, Yonsei University, Seoul 120-749 Korea

<sup>‡</sup>Department of Veterinary Medicine, Department of Biomedical Science and Technology, Konkuk University, Seoul 143-701 Korea

## S Supporting Information

**ABSTRACT:** Dual-modal fluorescent magnetic glyconanoparticles have been prepared and shown to be powerful in probing lectins displayed on pathogenic and mammalian cell surfaces. Blood group H1- and Le<sup>b</sup>-conjugated nanoparticles were found to bind to BabA displaying *Helicobacter pylori*, and Le<sup>a</sup>- and Le<sup>b</sup>-modified nanoparticles are both recognized by and internalized into DC-SIGN and SIGN-R1 expressing mammalian cells via lectin-mediated endocytosis. In addition, glyconanoparticles block adhesion of *H. pylori* to mammalian cells, suggesting that they can serve as inhibitors of infection of host cells by this pathogen. It has been also shown that owing to their magnetic properties, glyconanoparticles are useful tools to enrich lectin expressing cells. The combined results indicate that dual-modal glyconanoparticles are biocompatible and that they can be employed in lectin-associated biological studies and biomedical applications.



## INTRODUCTION

Multiple earlier studies have shown that interactions between glycans and carbohydrate binding proteins (lectins) displayed on the cell surface are involved in a variety of physiological and pathological processes.<sup>1</sup> For example, cell surface lectins in the immune system recognize glycans expressed on the exterior of pathogens, and these interactions lead to stimulation of immune responses to pathogens.<sup>2</sup> In addition, infections caused by pathogens, including *Helicobacter pylori* and influenza virus, takes place by initial adhesion of the pathogens to host cells through interactions of the pathogenic lectins (adhesins) with the host cell surface glycans.<sup>3</sup> Consequently, detection of cell surface lectins and an understanding of recognition events that take place between lectins and glycans are of great importance in both basic research and development of more efficacious drugs and diagnostic tools.

*H. pylori*, which colonizes the human stomach, is one of the most widespread infectious pathogens affecting nearly one-third of the world's population. *H. pylori* causes chronic gastritis, which may lead to peptic ulcer disease and gastric cancer.<sup>4</sup> The cell surface of this pathogen frequently contains adhesins that recognize specific host cell glycans,<sup>5</sup> as exemplified by the well-characterized blood group antigen-binding adhesin (BabA).<sup>6</sup> In this case, infection of hosts by *H. pylori* is triggered by binding of BabA to Le<sup>b</sup> present in the gastric mucosa. Because of their unique roles, *H. pylori* adhesins have been actively investigated. Because *H. pylori* strains express carbohydrate binding proteins on their surfaces, glycan-based detection methods have been

exploited as part of methods to diagnose diseases associated with this pathogen,<sup>7</sup> and materials that block associations of *H. pylori* with host glycans have been developed to prevent infections caused by this pathogen.<sup>8</sup>

Mammalian cells also express lectins on their surfaces. For instance, human DC-SIGN (dendritic cell-specific ICAM-3-grabbing nonintegrin) is a C-type lectin displayed on the surface of dendritic cells and macrophages.<sup>9</sup> Mouse SIGN-R1 (SIGN-related 1) is a homologue of human DC-SIGN that is expressed largely on macrophages in the splenic marginal zone and the medullar lymph nodes.<sup>10</sup> Two lectins recognize mannose-rich or fucosylated glycans in a Ca<sup>2+</sup>-dependent manner with subtle differences in their glycan binding properties.<sup>11,12</sup> When DC-SIGN and SIGN-R1 interact with glycans on host cells, bacteria or viruses, glycan antigens are internalized into cells via lectin-mediated endocytosis to induce immune activation. Because of their biological significance, mammalian cell surface lectins have been widely studied for an understanding of lectin-associated cellular processes.<sup>2,13</sup>

It is well-known that multivalent interactions of glycans with lectins enhance otherwise weak binding affinities of monomeric sugars to proteins.<sup>14</sup> Over a decade, glycan-conjugated nanoparticles have been constructed in biological and biomedical research efforts because they have high surface area-to-volume ratios in comparison to other glycoclusters, such

Received: January 19, 2015

Published: May 5, 2015

as neoglycopeptides, glycolipid micelles and glycoproteins, and thus provide higher lectin binding capacity.<sup>15</sup> Gold nanoparticles were first used as metal-based multivalent scaffolds to present glycan ligands.<sup>16</sup> Later, glycan-conjugated single-modal fluorescent<sup>17</sup> or magnetic nanoparticles<sup>7,18</sup> were prepared for detection and capture of lectin displaying cells as well as noninvasive imaging of glycan-protein recognition events in animals. Although single-modal glyconanoparticles have been prepared for glycan-associated biomedical and basic research, dual-modal glyconanoparticles that integrate the advantageous features of both fluorescent and magnetic properties have rarely been employed for these purposes.<sup>19</sup> In the study described below, we prepared oligosaccharide-conjugated dual-modal fluorescent magnetic nanoparticles (FMNPs) to probe mammalian and pathogenic cell surface lectins. The results of this effort show that dual-modal glyconanoparticles are useful tools in studies aimed at gaining an understanding of the biological roles of cell surface lectins, diagnosing pathogen-associated diseases and preventing pathogen infection.

## RESULTS AND DISCUSSION

**Preparation and Characterization of Glycan-Conjugated FMNPs.** FMNPs conjugated with multiple copies of three types of fucose-bearing oligosaccharides [Lewis a ( $Le^a$ ) and Lewis b ( $Le^b$ ) antigens and a blood group H type 1 (H1)] were constructed to target pathogenic and mammalian cell surface lectins (Figure 1). The required oligosaccharides were

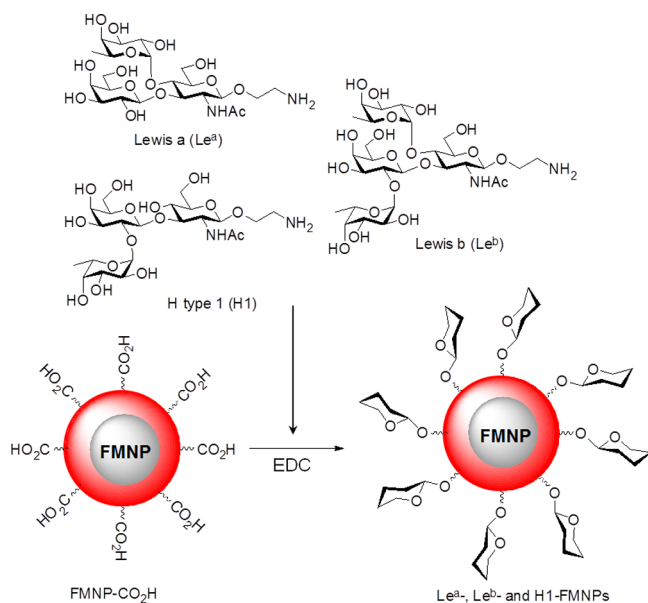


**Figure 1.** Preparation of glycan-conjugated dual-modal FMNPs.

synthesized in  $\beta$ -aminoethylated forms for conjugation to NPs as delineated in Scheme S1–S3.<sup>20</sup> The oligosaccharides were then coupled to carboxylic acid moieties on the FMNPs (a molar ratio of FMNPs to glycan = 1:30), which were composed of cobalt ferrite magnetic nanoparticles coated with a shell of amorphous silica containing rhodamine B isothiocyanate,<sup>21</sup> under amide coupling conditions to afford  $Le^a$ -,  $Le^b$ - and H1-FMNPs. Unreacted carboxylic acids on the NPs were then capped with 2-aminoethanol to suppress nonspecific adsorption during detection of cell-surface lectins.

The glycan-conjugated FMNPs were characterized by using FT-IR, Zeta potential, dynamic light scattering and trans-

mission electron microscopy (TEM) techniques. FT-IR spectra of glyconanoparticles showed the characteristic peaks of sugar (Figure S1), providing evidence that nanoparticles are successfully conjugated with sugars. The zeta potentials of nanoparticles were observed to change from  $-39$  mV to between  $-10$  and  $-15$  mV after coupling to oligosaccharides (Table S1). This result indicates that the negatively charged carboxylates of FMNPs are converted largely to amide moieties. The results of TEM imaging and dynamic light scattering analyses reveal that glyconanoparticles are well dispersed without forming severe aggregation as a result of the presence of hydrophilic glycans on their surface (Figure 2A and S2). In

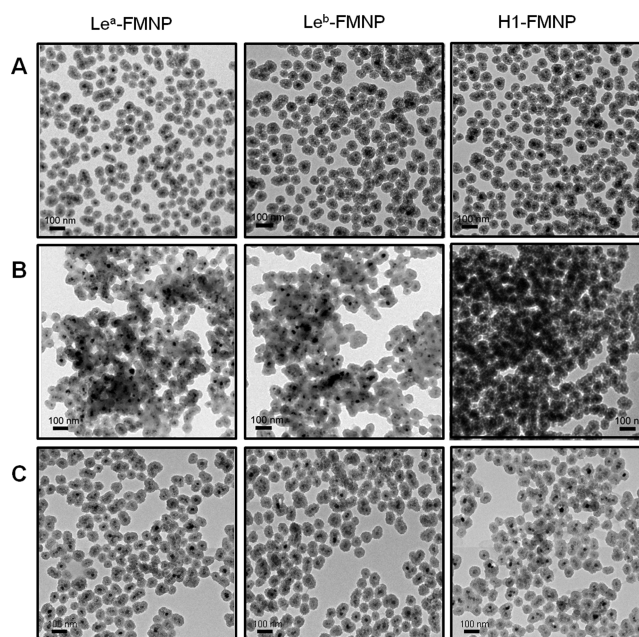


**Figure 2.** TEM images of glycan-conjugated FMNPs (A) before and after treatment with (B) AAL and (C) ConA (scale bar = 100 nm).

addition, the modified nanoparticles have a relatively homogeneous size distribution with average hydrodynamic diameters of ca. 80 nm. We also measured the efficiency of glycan conjugation to nanoparticles by labeling the unreacted carboxylic acids after glycan conjugation with a fluorescent dye Cy5. Approximately 80% carboxylic acids on the surface of nanoparticles were measured to be conjugated with three types of glycans (see Supporting Information).

To demonstrate that the glycans attached to FMNPs preserve their biological recognition activities, studies probing binding of the glyconanoparticles to lectins were conducted. TEM images show that the three glyconanoparticles form aggregates with *Aleuria aurantia* lectin (AAL), which is a fucose binding lectin,<sup>22</sup> owing to multivalent interactions with lectin (Figure 2B). In contrast, treatment with ConA, which is an  $\alpha$ -mannose/ $\alpha$ -glucose binding lectin, does not lead to the formation of aggregates of glyconanoparticles (Figure 2C).<sup>22</sup> Furthermore, analysis of lectin microarrays containing five lectins (ConA, AAL, wheat germ agglutinin; WGA, *Ricinus communis* agglutinin I; RCA<sub>120</sub> and Jacalin) after incubation with glyconanoparticles shows that only AAL recognizes three types of glyconanoparticles (Figure S3). Taken together, the results demonstrate that FMNPs are successfully modified with oligosaccharides and the resulting glyconanoparticles are selectively recognized by lectin.

**Fluorescent Detection and Magnetic Isolation of *H. pylori* with Glyconanoparticles.** Studies were performed to determine if the glycan-conjugated FMNPs can be employed to fluorescently detect *H. pylori*. First, expression of BabA in the two *H. pylori* strains, J99 and 26695, was examined by reverse transcription-polymerase chain reaction (RT-PCR). The results indicate that *H. pylori* J99 expresses a BabA gene but *H. pylori* 26695 does not (Figure S4).<sup>23</sup> In order to evaluate their ability to recognize cell surface BabA, the individual glyconanoparticles (100  $\mu\text{g/mL}$ ) were incubated for 1 h with *H. pylori* J99, which was pretreated for 5 min with 1  $\mu\text{M}$  Hoechst 33342 for bacterial cell staining. In control experiments, *H. pylori* 26695 was incubated with the glyconanoparticles under the same conditions. Analysis of confocal microscopy images shows that whereas Le<sup>b</sup>- and H1-FMNPs but not Le<sup>a</sup>-FMNPs bind to BabA expressing J99, the three glyconanoparticles do not bind to BabA lacking 26695 (Figure 3 and Figure S5). To evaluate

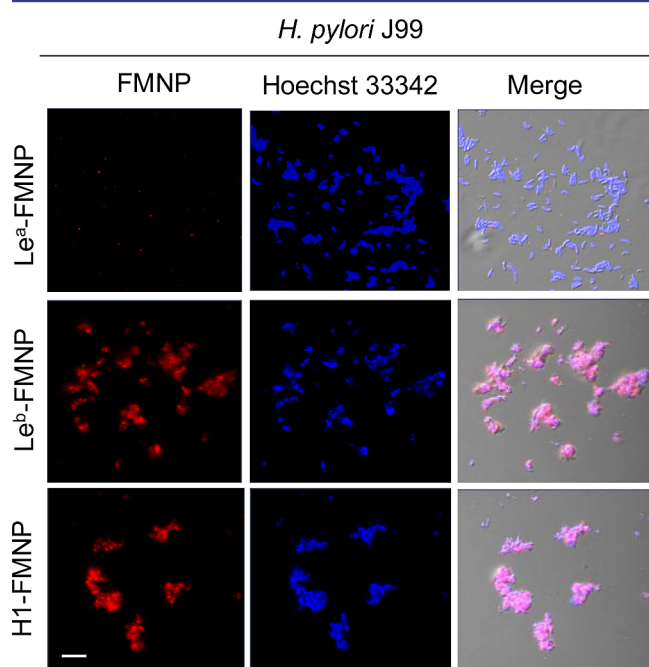


**Figure 3.** Binding of glyconanoparticles to *H. pylori* J99. J99 cells pretreated with 1  $\mu\text{M}$  Hoechst 33342 for 5 min were incubated with 100  $\mu\text{g/mL}$  of glyconanoparticles for 1 h. After washing, images were obtained using confocal microscopy (scale bar = 10  $\mu\text{m}$ ).

the binding affinities of glycan-conjugated FMNPs to *H. pylori*, surface plasmon resonance (SPR) assays were conducted using a sensor chip immobilized by three types of glyconanoparticles. SPR analysis reveals that BabA expressing J99 cells bind to Le<sup>b</sup>-FMNPs more strongly than H1-FMNPs but interact with Le<sup>a</sup> very weakly (Figure S6), a phenomenon which is consistent with the previous results.<sup>6a,24</sup>

We investigated the effect of sugar densities on the surface of nanoparticles on binding to AAL and *H. pylori*. For this purpose, FMNPs were conjugated with glycans at various molar ratios (a molar ratio of FMNPs to glycan = 1:5, 1:10, 1:20 and 1:30). Analysis of confocal microscope images of J99 cells incubated with glyconanoparticles show that NPs with the higher glycan density lead to more aggregation of cells via multivalent interactions (Figure S7). Lectin microarray analysis probed with glyconanoparticles also reveals that more densely conjugated glyconanoparticles have the stronger binding affinity

to AAL (Figure S8). In particular, glyconanoparticles prepared at a 1:30 molar ratio were found to provide the reproducible and reliable binding data for protein and cell experiments.

As the dual-modal glyconanoparticles in this effort are magnetic, they have the potential of being applicable in magnetic methods for the isolation of adhesin displaying pathogens. To demonstrate this potential, *H. pylori* strains J99 and 26695 were incubated separately with the three types of glyconanoparticles (100  $\mu\text{g/mL}$ ) for 1 h. A magnetic field was applied to each mixture for 0.5 h. Only J99 cells that were treated with Le<sup>b</sup>- and H1-FMNPs were collected by using the magnet (Figure S9A). For the purpose of separating adhesin expressing cells from lacking cells, a mixture of *H. pylori* J99 and lectin lacking *E. coli* HB101 was incubated with 100  $\mu\text{g/mL}$  Le<sup>b</sup>-FMNPs for 0.5 h and then subjected to a magnetic field. The separated cells were subjected to RT-PCR with a BabA gene in order to determine if two different cell types are separated. As shown in Figure S9B, Le<sup>b</sup>-FMNP bound cells were found to express this gene but unbound cells exhibit little expression of the gene, indicating that glyconanoparticles can be used to enrich adhesin expressing pathogens.

**Blocking Adhesion of *H. pylori* to Mammalian Cells Using Glyconanoparticles.** Next, we tested the feasibility of glyconanoparticles to block adhesion of *H. pylori* to mammalian cells. Toward this end, AGS cells (human gastric carcinoma cells) were incubated with *H. pylori* J99 for 0.5 h and then the mixture was treated for 1 h with Le<sup>b</sup>- and H1-FMNPs at a concentration of 100  $\mu\text{g/mL}$ , where glyconanoparticles have no cytotoxicity against AGS cells (Figure S10), in order to monitor adhered pathogenic cells. Analysis of confocal microscope images shows that *H. pylori* J99 adheres to the mammalian cells (Figure 4A).<sup>25</sup> The results of an experiment in which AGS cells were incubated with glyconanoparticles (100  $\mu\text{g/mL}$ ) for 1 h show that the glyconanoparticles neither bind to nor are internalized into AGS cells (Figure S11). Then, to investigate the effect of glyconanoparticles on suppression of adhesion of *H. pylori* to mammalian cells, AGS cells were incubated for 0.5 h with *H. pylori* J99 in the presence of Le<sup>b</sup>- or H1-FMNPs at a concentration of 500  $\mu\text{g/mL}$ , where glyconanoparticles have no cytotoxicity against AGS cells (Figure S10). Inspection of the images shows that most pathogenic cells do not bind to mammalian cells in the presence of glyconanoparticles (Figure 4B and S12). This observation indicates that glyconanoparticles are efficacious in blocking adhesion of *H. pylori* to mammalian cells. Taken together, the results suggest that glyconanoparticles can serve as useful agents to detect and isolate adhesin displaying pathogens and to block infection of pathogens in host cells.

**Uptake of Glyconanoparticles by DC-SIGN and SIGN-R1 Expressing Mammalian Cells.** We next turned our attention to determine if glycan-conjugated FMNPs can be employed to detect mammalian cell surface lectins. To test this, glyconanoparticles (200  $\mu\text{g/mL}$ ) were exposed for 3 h to DCEK cells stably expressing human DC-SIGN (DCEK-DC-SIGN) and mouse SIGN-R1 (DCEK-SIGN-R1) in the presence or absence of 200  $\mu\text{g/mL}$  mannan (Figure S13), a tight binding ligand of DC-SIGN and SIGN-R1.<sup>26</sup> As a control wild-type DCEK cells lacking these lectins were also incubated with glyconanoparticles. Analysis of confocal microscope images shows that strong red fluorescence arises from the insides of DCEK-DC-SIGN and DCEK-SIGN-R1 cells after treatment with Le<sup>a</sup>- and Le<sup>b</sup>-FMNPs (Figure 5), indicating that the glyconanoparticles are internalized into these cells after they

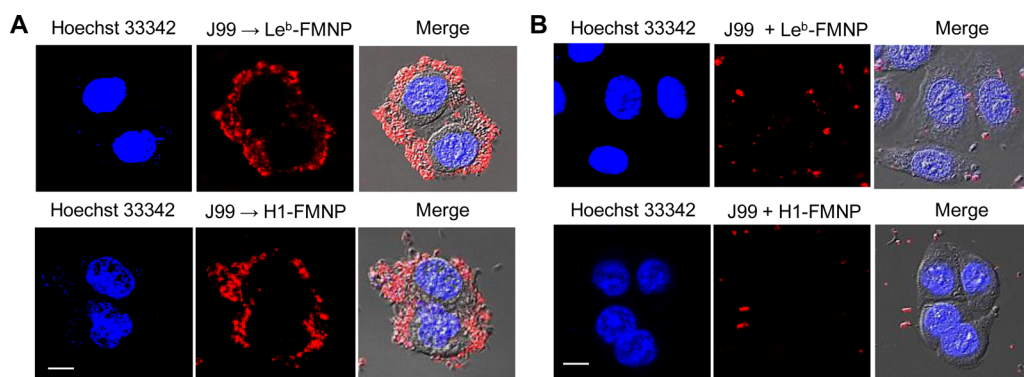


**Figure 4.** Glyconanoparticles block adhesion of *H. pylori* J99 to mammalian cells. (A) AGS cells, pretreated for 5 min with 1  $\mu$ M Hoechst 33342 for staining the nucleus, were incubated with J99 for 0.5 h. J99 cells adhered to AGS cells were detected by treatment with 100  $\mu$ g/mL of (top) Le<sup>b</sup>- and (bottom) H1-FMNPs for 1 h. (B) AGS cells, pretreated with 1  $\mu$ M Hoechst 33342 for 5 min, were incubated with J99 for 0.5 h in the presence of 500  $\mu$ g/mL of (top) Le<sup>b</sup>- and (bottom) H1-FMNPs. Images were obtained using confocal microscopy (scale bar = 10  $\mu$ m).

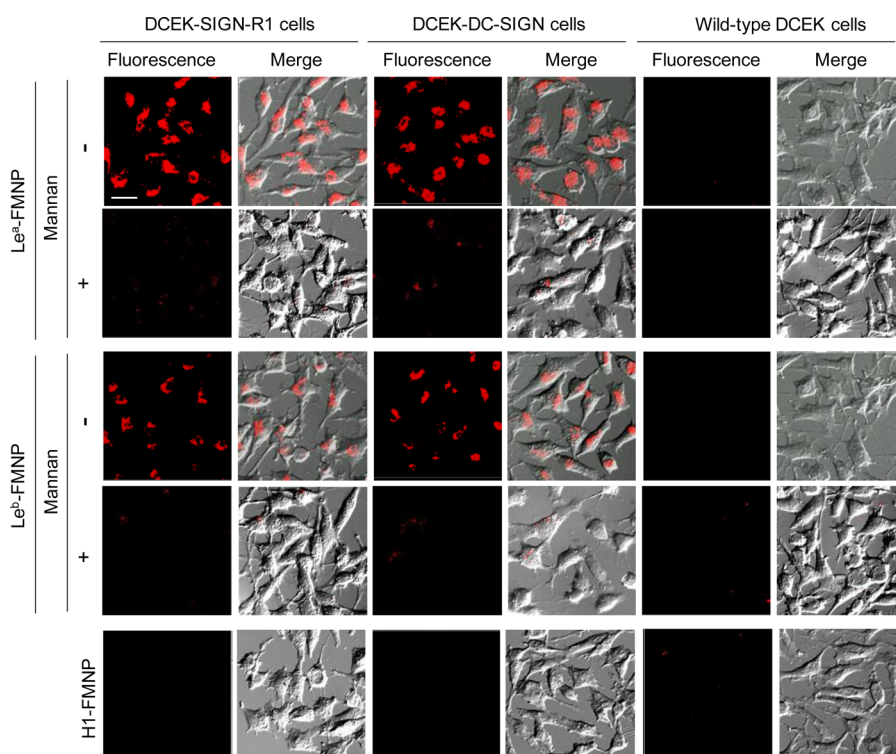


**Figure 5.** Detection of lectins expressed on mammalian cell surfaces with glyconanoparticles. DCEK-SIGN-R1 and DCEK-DC-SIGN cells were treated with 200  $\mu$ g/mL of Le<sup>a</sup>- or Le<sup>b</sup>-FMNPs for 3 h in the presence or absence of 200  $\mu$ g/mL mannan as a competitor. Images were obtained using confocal microscopy (scale bar = 20  $\mu$ m).

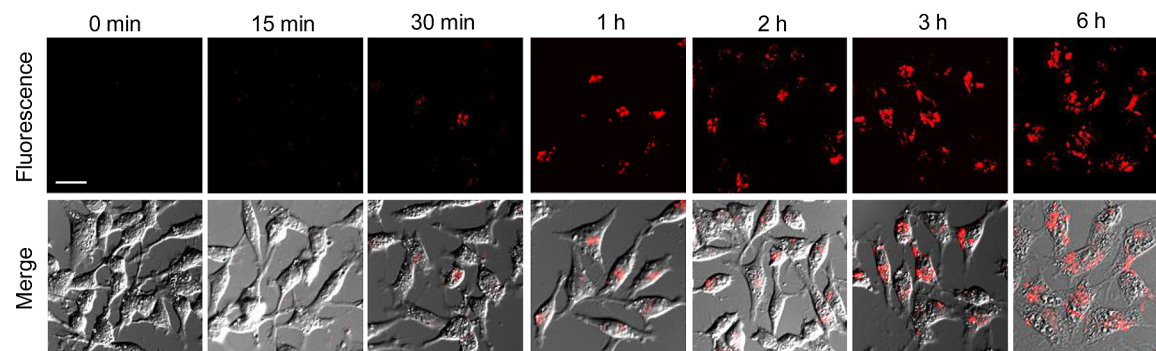


**Figure 6.** Time-dependent uptake of Le<sup>a</sup>-FMNPs by DCEK-DC-SIGN cells. The cells were incubated with 200  $\mu$ g/mL of Le<sup>a</sup>-FMNPs during a given time period. After washing, images were obtained using confocal microscopy (scale bar = 20  $\mu$ m).

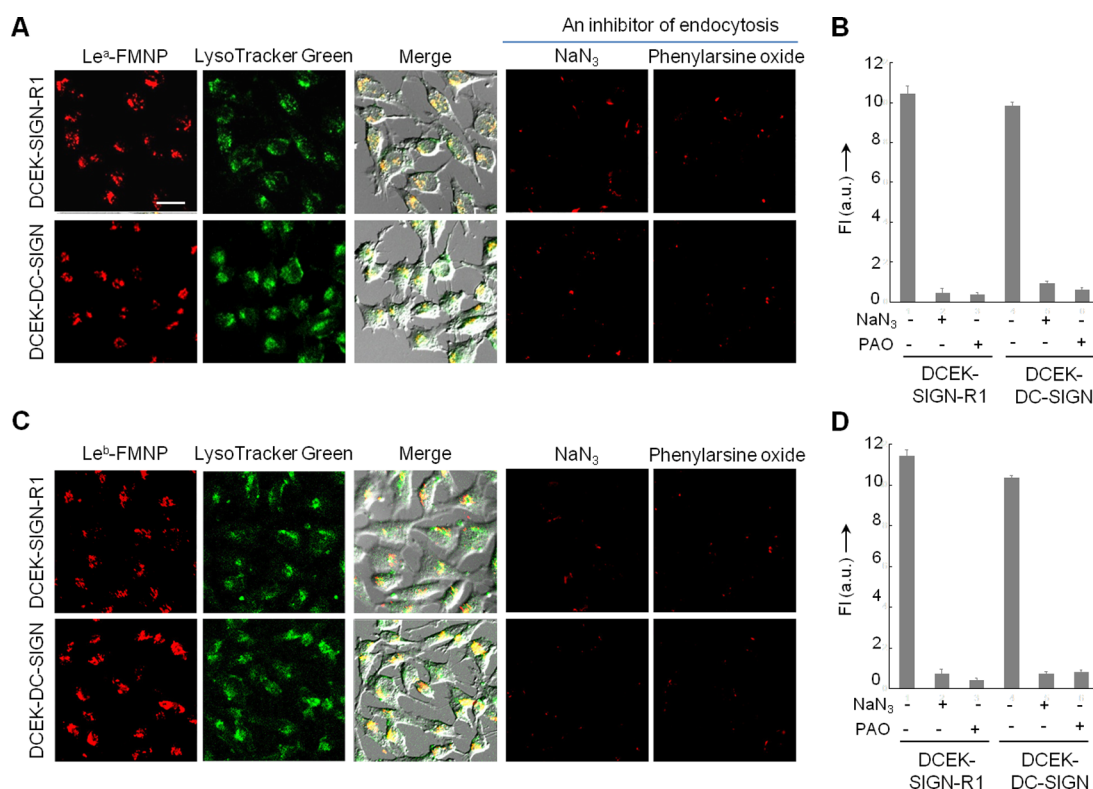


**Figure 7.** Glyconanoparticles are internalized into cells via lectin-mediated endocytosis. (Left three images) DCEK-SIGN-R1 and DCEK-DC-SIGN cells were treated with 200  $\mu\text{g}/\text{mL}$  of (A) Le<sup>a</sup>- and (C) Le<sup>b</sup>-FMNPs for 3 h in the presence of 50 nM LysoTracker Green. Images were obtained using confocal microscopy. (Right two images) The cells were pretreated with either 250 nM phenylarsine oxide or 0.05% w/v NaN<sub>3</sub> for 1 h and then incubated with 200  $\mu\text{g}/\text{mL}$  of (A) Le<sup>a</sup>- and (C) Le<sup>b</sup>-FMNPs for 3 h at 37 °C. Images were obtained using confocal microscopy (scale bar = 20  $\mu\text{m}$ ). Quantitative data of fluorescence intensity of (B) Le<sup>a</sup>- and (D) Le<sup>b</sup>-FMNPs in cells.

bind to cell surface lectins.<sup>11,12</sup> However, when mannan is present, fluorescence intensity in lectin displaying cells is greatly attenuated. Importantly, very weak fluorescence is observed in wild-type DCEK cells treated with glyconanoparticles as well as DCEK-DC-SIGN and DCEK-SIGN-R1 cells treated with H1-FMNPs. The results of time-dependent studies show that fluorescence comes from lectin expressing cells 30 min after the start of incubation with glyconanoparticles (Figure 6). Taken together, the results demonstrate that nanoparticle binding specifically results from interactions of carbohydrates with cell surface lectins.

To test if glyconanoparticles are taken up by cells via lectin-mediated endocytosis, DCEK-DC-SIGN-R1 and DCEK-DC-SIGN cells were incubated with 200  $\mu\text{g}/\text{mL}$  of Le<sup>a</sup>- or Le<sup>b</sup>-FMNPs for 3 h and then treated with 50 nM LysoTracker Green for 1 h. The fluorescence signals arising from the glyconanoparticles overlap for the most part with those of LysoTracker (Figure 7). To confirm this conclusion, the effect of an endocytosis inhibitor on cellular uptake of glyconanoparticles was investigated. For this purpose, DCEK-SIGN-R1 and DCEK-DC-SIGN cells were treated for 1 h with either 250 nM phenylarsine oxide (PAO) or 0.05% w/v NaN<sub>3</sub>, both of which are known inhibitors of endocytosis.<sup>27</sup> The cells were then incubated with 200  $\mu\text{g}/\text{mL}$  of Le<sup>a</sup>- or Le<sup>b</sup>-FMNPs for 3 h. Uptake of glyconanoparticles by the cells was observed to be markedly reduced in the presence of either inhibitor (Figure 7), demonstrating that cellular uptake of glyconanoparticles takes place via lectin-mediated endocytosis.

Then, experiments were performed to enrich lectin expressing mammalian cells using a magnet. The results show

that Le<sup>a</sup>- or Le<sup>b</sup>-FMNP treated DCEK-SIGN-R1 and DCEK-DC-SIGN cells can be efficiently collected by using a magnet and that the collection is suppressed in the presence of 200  $\mu\text{g}/\text{mL}$  mannan (Figure S14). In contrast, neither H1-FMNP treated DCEK-SIGN-R1 and DCEK-DC-SIGN cells nor Le<sup>a</sup>- and Le<sup>b</sup>-FMNP treated wild-type DCEK cells are not enriched by employing this method.

**ROS Production of DC-SIGN and SIGN-R1 Expressing Cells by Glyconanoparticles.** Observations made in previous studies show that binding of glycan ligands to DC-SIGN and SIGN-R1 cells induces the production of reactive oxygen species (ROS).<sup>28</sup> To evaluate if glyconanoparticle treated cells also generate ROS after binding to lectin expressing cells, DCEK-DC-SIGN-R1, DCEK-DC-SIGN and wild-type DCEK cells were treated with 40  $\mu\text{M}$  of a boronate-based fluorescent H<sub>2</sub>O<sub>2</sub> probe<sup>29</sup> for 1 h and then incubated with 200  $\mu\text{g}/\text{mL}$  of Le<sup>a</sup>- or Le<sup>b</sup>-FMNPs for 3 h. Glyconanoparticle treated DC-SIGN and SIGN-R1 expressing cells display intense fluorescence signals arising from the probe, indicating that H<sub>2</sub>O<sub>2</sub> is generated (Figure 8). Similar results arose when cells were treated with 200  $\mu\text{g}/\text{mL}$  mannan as a positive control (Figure S15). In contrast, wild-type DCEK cells do not produce H<sub>2</sub>O<sub>2</sub> under the same conditions. These results demonstrate that glyconanoparticles act as functional ligands in lectin displaying cells. Although great progress has been made in understanding of DC-SIGN mediated biological processes, the functions of SIGN-R1 have not been well-elucidated in comparison to those of DC-SIGN. Therefore, it is expected that glyconanoparticles could serve as useful probes for studies of the biological roles played by SIGN-R1.

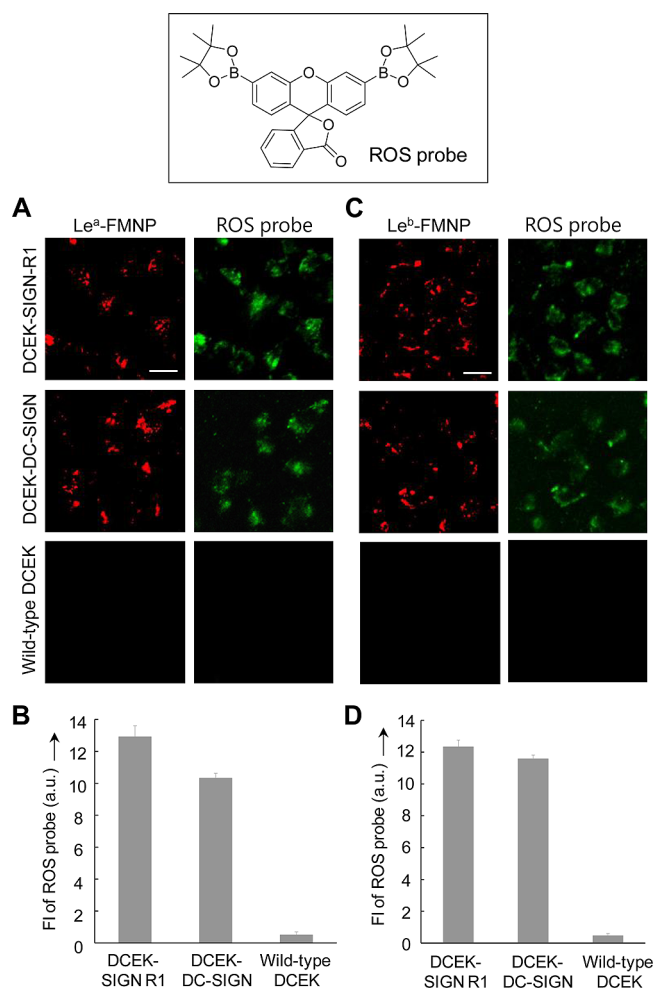


**Figure 8.** Production of ROS in mammalian cells treated with glyconanoparticles. DCEK-SIGN-R1, DCEK-DC-SIGN and wild-type DCEK cells were treated with 40  $\mu\text{M}$  ROS probe for 1 h and then incubated with 200  $\mu\text{g}/\text{mL}$  of (A)  $\text{Le}^{\text{a}}$ - and (C)  $\text{Le}^{\text{b}}$ -FMNPs for 3 h. Images were obtained using confocal microscopy (scale bar = 20  $\mu\text{m}$ ). Quantitative data of fluorescence intensity of the ROS probe in cells treated with (B)  $\text{Le}^{\text{a}}$ - and (D)  $\text{Le}^{\text{b}}$ -FMNPs.

## CONCLUSION

We have constructed and successfully applied dual-modal fluorescent magnetic glyconanoparticles to probe lectins displayed on pathogenic and mammalian cell surfaces. Using fluorescent cell imaging, we have demonstrated that dual-modal glyconanoparticles serve as useful probes to detect mammalian and pathogenic cells, which present specific lectins on their surfaces. In addition, it has been also shown that dual-modal glyconanoparticles are useful tools to enrich lectin expressing cells owing to their magnetic properties. Interestingly, our results show that the glyconanoparticles can be used as agents to block binding of adhesin expressing *H. pylori* to mammalian cells. The combined observations suggest that dual-modal glyconanoparticles have great potential for aiding an understanding of biological roles played by lectins and for diagnosing and/or preventing pathogen associated diseases. Consequently, multivalent glyconanoparticles should have applications that go beyond basic studies of glycan-lectin interactions.

## EXPERIMENTAL SECTION

**Preparation of  $\text{Le}^{\text{a}}$ ,  $\text{Le}^{\text{b}}$ - and H1-FMNPs.** FMNPs (TMSR50, Biterials, Korea; cobalt ferrite magnetic nanoparticles coated with a shell of amorphous silica containing rhodamine B isothiocyanate, the saturation magnetization;  $\pm 33.5$  emu/g at 273 K and  $\pm 1$  T) were washed twice and redispersed with 10 mM sodium bicarbonate buffer (pH 8.7) under sonication. FMNPs were reacted with  $\text{Le}^{\text{a}}$ ,  $\text{Le}^{\text{b}}$  or H1 in the presence of *N*-ethyl-*N'*-dimethylaminopropyl carbodiimide HCl (EDC) at room temperature with shaking (a molar ratio, FMNPs:oligosaccharide:EDC = 1:30:200). After 2 h, ethanolamine solution (3% in 10 mM sodium bicarbonate, pH 8.7) was added to the mixture in order to cap remaining activated carboxyl groups. The glycan-conjugated FMNP mixture was centrifuged at 15 000 rpm for 10 min and washed with water to remove the remaining reagents. This washing cycle was repeated 5 times, after which the conjugated FMNPs were resuspended in water with the aid of sonication. The final concentrations of  $\text{Le}^{\text{a}}$ ,  $\text{Le}^{\text{b}}$ - and H1-FMNPs are ca. 2 mg/mL.

**Fourier Transform Infrared (FT-IR) Spectroscopy.** The mid-IR absorbance spectra (800–4000  $\text{cm}^{-1}$ ) were recorded on a FT-IR spectrometer (Vertex70, Bruker) equipped with a deuterated L-alanine doped triglycene sulfate detector at room temperature. The spectral resolution was 4  $\text{cm}^{-1}$  and 128 scans were collected for each spectrum. The background spectrum of air was obtained as a reference. The glycan-conjugated FMNPs were measured on the ZnSe ATR crystal plate.

**Measurements of Zeta Potential and Hydrodynamic Size.** In a typical measurement, 200  $\mu\text{L}$  of glycan-conjugated FMNPs (2 mg/mL in water) was diluted in 1.8 mL of water and homogeneously resuspended with the aid of sonication under an ice bath for 10 min. Zeta potential and hydrodynamic size of glyconanoparticles were measured using the Zetasizer (Malvern Instrument, UK) and a minimum of three measurements per sample were made at 25  $^{\circ}\text{C}$ .

**Transmission Electron Microscopy (TEM).** In a typical measurement, 2  $\mu\text{L}$  glyconanoparticle sample (500  $\mu\text{g}/\text{mL}$  in water) was deposited on ultrathin-carbon type A, 300 mesh copper grids (Ted Pella, Inc.) and left to dry at room temperature overnight before visualizing with TEM. For aggregation studies of glycan-conjugated FMNP induced by lectin, glyconanoparticle sample (500  $\mu\text{g}/\text{mL}$  in water) was mixed together with AAL or ConA (0.5  $\mu\text{g}/\text{mL}$ ) in 10 mM sodium bicarbonate buffer (pH 8.7) at room temperature. It was left to incubate at the same temperature for 3 h, and then the mixture was deposited on ultrathin-carbon type A, 300 mesh copper grids and left to dry at room temperature overnight. TEM images were collected on a JEM-2010 operating at 200 kV using Gatan multiscan CCD camera with Digital Micrograph imaging software.

**Cell Culture.** *H. pylori* strains 26695 and J99 (*H. pylori* Korean Type Culture Collection, HpKTCC, Gyeongsang National University) were grown on Brucella broth agar base plates (Neogen Corporation) supplemented with 2.5% (w/v) Bacto-Agar (Becton, Dickinson and company) and 10% (v/v) heat-inactivated horse serum. *H. pylori* cells were cultured under microaerophilic conditions (3%  $\text{O}_2$ , 10%  $\text{CO}_2$  and 87%  $\text{N}_2$ ) at 37  $^{\circ}\text{C}$  for 1 day before use. Wild-type DCEK, DCEK-DC-SIGN, DCEK-SIGN-R1 and AGS cells (human gastric adenocarcinoma epithelial cells) were cultured in RPMI 1640 supplemented with 10% fetal bovine serum (FBS), 50 units/mL of penicillin and 50  $\mu\text{g}/\text{mL}$  of streptomycin at 37  $^{\circ}\text{C}$  in a humidified incubator with 5%  $\text{CO}_2$ .

**Detection of *H. pylori* with Glyconanoparticles.** *H. pylori* strains J99 and 26695 ( $10^6$  cells) in PBS were treated with 1  $\mu\text{M}$  Hoechst 33342 for 5 min. The cells were centrifuged and washed with PBS. The stained bacterial cells in PBS were incubated with 100  $\mu\text{g}/\text{mL}$  of  $\text{Le}^{\text{a}}$ ,  $\text{Le}^{\text{b}}$ - or H1-FMNPs for 1 h at room temperature. After washing, images were obtained using confocal microscopy (LSM 700 META, Carl Zeiss, Germany).

**Adhesion of *H. pylori* to Mammalian Cells.** AGS cells ( $2 \times 10^4$  cells) in culture media were treated with 1  $\mu\text{M}$  Hoechst 33342 for 5 min for staining the nucleus. After washing with culture media, the cells in culture media were incubated with *H. pylori* J99 ( $2 \times 10^7$  cells) for 0.5 h at 37  $^{\circ}\text{C}$ . After washing with PBS, the cells were incubated with 100  $\mu\text{g}/\text{mL}$  glyconanoparticles for 1 h to fluorescently detect

adhered bacterial cells. After washing with PBS, cell images were obtained using confocal microscopy.

**Blocking of Adhesion of *H. pylori* to Mammalian Cells by Glyconanoparticles.** *H. pylori* J99 cells ( $2 \times 10^7$  cells) in PBS were treated with 1  $\mu$ M Hoechst 33342 for 5 min. After washing with PBS, cells in PBS were incubated with 500  $\mu$ g/mL of Le<sup>b</sup>- or H1-FMNPs for 1 h and then the mixture was added to AGS cells ( $2 \times 10^4$  cells) in culture media. After incubation for 0.5 h, cell images were obtained using confocal microscopy after washing with PBS.

**Separation of Glyconanoparticle-Bound *H. pylori* Cells with a Magnet.** A mixture of *H. pylori* J99 and *E. coli* HB101 was incubated with 100  $\mu$ g/mL of glyconanoparticles for 1 h. A magnetic field was applied to the mixture with a magnet for 0.5 h. Fluorescence images were obtained using a G:BOX Chemi Fluorescent and Chemiluminescent Imaging System (Syngene).

**Uptake of Glyconanoparticles by Cells.** Wild-type DCEK, DCEK-DC-SIGN and DCEK-SIGN-R1 cells ( $2 \times 10^4$  cells) were separately incubated with 200  $\mu$ g/mL of Le<sup>a</sup>-, Le<sup>b</sup>- or H1-FMNPs in culture media for 3 h at 37 °C. After washing twice with PBS to remove the remaining nanoparticles, bright field and fluorescence images of the cells were obtained using confocal microscopy.

For the mannan competition study, wild-type DCEK, DCEK-DC-SIGN and DCEK-SIGN-R1 cells ( $2 \times 10^4$  cells) were pretreated with 200  $\mu$ g/mL mannan in culture media at 37 °C. After 1 h, the cells were treated with 200  $\mu$ g/mL of Le<sup>a</sup>-, Le<sup>b</sup>- or H1-FMNPs in culture media for 3 h at 37 °C. After washing with PBS twice, the treated cells were imaged by using confocal microscopy.

**Study of Lectin-Mediated Endocytosis.** Wild-type DCEK, DCEK-DC-SIGN and DCEK-SIGN-R1 cells ( $2 \times 10^4$  cells) were incubated with 200  $\mu$ g/mL of Le<sup>a</sup>-, Le<sup>b</sup>- or H1-FMNPs in culture media for 3 h at 37 °C. After washing twice with PBS, the cells were incubated with 50 nM LysoTracker Green (Invitrogen) in culture media for 1 h at 37 °C. After washing twice with PBS, bright field and fluorescence images of the cells were obtained using confocal microscopy.

For the endocytosis inhibition study, DCEK-DC-SIGN and DCEK-SIGN-R1 cells ( $2 \times 10^4$  cells) were pretreated with either 250 nM phenylarsine oxide or 0.05% w/v NaN<sub>3</sub> for 1 h and then incubated with 200  $\mu$ g/mL of Le<sup>a</sup>- or Le<sup>b</sup>-FMNPs in culture media for 3 h at 37 °C. After washing twice with PBS, the treated cells were imaged by using confocal microscopy.

**ROS Production of Cells by Glycan-Conjugated FMNPs.** Wild-type DCEK, DCEK-DC-SIGN and DCEK-SIGN-R1 cells ( $2 \times 10^4$  cells) were incubated with 40  $\mu$ M of a boronate-based ROS probe in culture media without phenol red for 1 h at 37 °C. After washing twice with PBS to remove the remaining ROS probe, the cells were incubated with 200  $\mu$ g/mL of Le<sup>a</sup>-, Le<sup>b</sup>- or H1-FMNPs in culture media for 3 h at 37 °C. After washing twice with PBS, the treated cells were imaged by using confocal microscopy.

## ■ ASSOCIATED CONTENT

### Ⓢ Supporting Information

Synthetic details, experimental procedures, NMR data and Figure S1–S15. The Supporting Information is available free of charge on the ACS Publications website at DOI: 10.1021/jacs.5b00592.

## ■ AUTHOR INFORMATION

### Corresponding Author

\*injae@yonsei.ac.kr

### Author Contributions

<sup>§</sup>The first two authors (S.P. and G.-H.K.) contributed equally to this work.

### Notes

The authors declare no competing financial interest.

## ■ ACKNOWLEDGMENTS

This work was supported by the National Creative Research Initiative (2010-0018272) program in Korea. We acknowledge Wook Jang for early involvement in the project and Cheol Wan Park for synthesis of a ROS fluorescent probe.

## ■ REFERENCES

- (1) (a) Varki, A. *Glycobiology* **1993**, *3*, 97–130. (b) Bertozzi, C. R.; Kiessling, L. L. *Science* **2001**, *291*, 2357–2364. (c) Park, S.; Lee, M.-R.; Shin, I. *Chem. Soc. Rev.* **2008**, *37*, 1579–1591. (d) Banerjee, P. S.; Hart, G. W.; Cho, J. W. *Chem. Soc. Rev.* **2013**, *42*, 4345–4357.
- (2) (a) Crocker, P. R. *Curr. Opin. Pharmacol.* **2005**, *5*, 431–437. (b) van Kooyk, Y.; Rabinovich, G. A. *Nat. Immunol.* **2008**, *9*, 593–601. (c) Crocker, P. R.; Paulson, J. C.; Varki, A. *Nat. Rev. Immunol.* **2007**, *7*, 255–266. (d) Weis, W. I.; Taylor, M. E.; Drickamer, K. *Immunol. Rev.* **1998**, *163*, 19–34.
- (3) (a) Smith, A. E.; Helenius, A. *Science* **2004**, *304*, 237–242. (b) Imberty, A.; Varrot, A. *Curr. Opin. Struct. Biol.* **2008**, *18*, 567–576.
- (4) (a) Covacci, A.; Telford, J. L.; Giudice, G. D.; Parsonnet, J.; Rappuoli, R. *Science* **1999**, *284*, 1328–1333. (b) Polk, D. B., Jr.; Peek, R. M. *Nat. Rev. Cancer* **2010**, *10*, 403–414.
- (5) Oleastro, M.; Ménard, A. *Biology* **2013**, *2*, 1110–1134.
- (6) (a) Aspholm-Hurtig, M.; Dailide, G.; Lahmann, M.; Kalia, A.; Ilver, D.; Roche, N.; Vikström, S.; Sjöström, R.; Lindén, S.; Bäckström, A.; Lundberg, C.; Arnqvist, A.; Mahdavi, J.; Nilsson, U. J.; Velapatiño, B.; Gilman, R. H.; Gerhard, M.; Alarcon, T.; López-Brea, M.; Nakazawa, T.; Fox, J. G.; Correa, P.; Dominguez-Bello, M. G.; Perez-Perez, G. I.; Blaser, M. J.; Normark, S.; Carlstedt, I.; Oscarson, S.; Teneberg, S.; Berg, D. E.; Borén, T. *Science* **2004**, *305*, 519–522. (b) Ilver, D.; Arnqvist, A.; Ogren, J.; Frick, I. M.; Kersulyte, D.; Incecik, E. T.; Berg, D. E.; Covacci, A.; Engstrand, L.; Borén, T. *Science* **1998**, *279*, 373–377.
- (7) Rouhanifard, S. H.; Xie, R.; Zhang, G.; Sun, X.; Chen, X.; Wu, P. *Biomacromolecules* **2012**, *13*, 3039–3045.
- (8) Lin, Y. H.; Tsai, S. C.; Lai, C. H.; Lee, C. H.; He, Z. S.; Tseng, G. C. *Biomaterials* **2013**, *34*, 4466–4479.
- (9) (a) Geijtenbeek, T. B.; Kwon, D. S.; Torensma, R.; van Vliet, S. J.; van Duijnhoven, G. C.; Middel, J.; Cornelissen, I. L.; Nottet, H. S.; KewalRamani, V. N.; Littman, D. R.; Figdor, C. G.; van Kooyk, Y. *Cell* **2000**, *100*, 587–597. (b) Geijtenbeek, T. B.; Torensma, R.; van Vliet, S. J.; van Duijnhoven, G. C.; Adema, G. J.; van Kooyk, Y.; Figdor, C. G. *Cell* **2000**, *100*, 575–585.
- (10) Kang, Y. S.; Yamazaki, S.; Iyoda, T.; Pack, M.; Bruening, S. A.; Kim, J. Y.; Takahara, K.; Inaba, K.; Steinman, R. M.; Park, C. G. *Int. Immunol.* **2003**, *15*, 177–186.
- (11) Guo, Y.; Feinberg, H.; Conroy, E.; Mitchell, D. A.; Alvarez, R.; Blixt, O.; Taylor, M. E.; Weis, W. I.; Drickamer, K. *Nat. Struct. Mol. Biol.* **2004**, *11*, 591–598.
- (12) Galustian, C.; Park, C. G.; Chai, W.; Kiso, M.; Bruening, S. A.; Kang, Y.-S.; Steinman, R. M.; Feizi, T. *Int. Immunol.* **2004**, *16*, 853–866.
- (13) Lepenies, B.; Lee, J.; Sonkaria, S. *Adv. Drug Delivery Rev.* **2013**, *65*, 1271–1281.
- (14) (a) Lundquist, J. J.; Toone, E. J. *Chem. Rev.* **2002**, *102*, 555–578. (b) Kiessling, L. L.; Gestwicki, J. E.; Strong, L. E. *Angew. Chem., Int. Ed.* **2006**, *45*, 2348–2368. (c) Tian, X.; Pai, J.; Baek, K.-H.; Ko, S.-K.; Shin, I. *Chem.—Asian J.* **2011**, *6*, 2107–2113. (d) Lee, M.-R.; Jung, D.-W.; Williams, D.; Shin, I. *Org. Lett.* **2005**, *7*, 5477–5480. (e) Mammen, M.; Choi, S.-K.; Whitesides, G. M. *Angew. Chem., Int. Ed.* **1998**, *37*, 2754–2794. (f) Tian, X.; Baek, K.-H.; Shin, I. *Mol. Biosyst.* **2013**, *9*, 978–986. (g) Lee, M. M.; Childs-Disney, J. L.; Pushechnikov, A.; French, J. M.; Sobczak, K.; Thornton, C. A.; Disney, M. D. *J. Am. Chem. Soc.* **2009**, *131*, 17464–17472. (h) Lee, M. M.; Pushechnikov, A.; Disney, M. D. *ACS Chem. Biol.* **2009**, *4*, 345–355. (i) Wittmann, V.; Seeberger, S. *Angew. Chem., Int. Ed.* **2000**, *39*, 4348–4352. (j) Schwefel, D.; Maierhofer, C.; Beck, J. G.; Seeberger, S.; Diederichs, K.; Möller, H. M.; Welte, W.; Wittmann, V. *J. Am. Chem. Soc.* **2010**, *132*, 8704–8719. (k) Koshi, Y.; Nakata, E.; Miyagawa, M.;

- Tsukiji, S.; Ogawa, T.; Hamachi, I. *J. Am. Chem. Soc.* **2008**, *130*, 245–251. (l) Tian, X.; Pai, J.; Shin, I. *Chem.—Asian J.* **2012**, *7*, 2052–2060. (m) Murthy, B. N.; Voelcker, N. H.; Jayaraman, N. *Glycobiology* **2006**, *16*, 822–832. (n) Frison, N.; Taylor, M. E.; Soilleux, E.; Bousser, M. T.; Mayer, R.; Monsigny, M.; Drickamer, K.; Roche, A. C. *J. Biol. Chem.* **2003**, *278*, 23922–23929. (o) Chen, X.; Tam, U. C.; Czapinski, J. L.; Lee, G. S.; Rabuka, D.; Zettl, A.; Bertozzi, C. R. *J. Am. Chem. Soc.* **2006**, *128*, 6292–6293. (p) Pasparakis, G.; Alexander, C. *Angew. Chem., Int. Ed.* **2008**, *47*, 4847–4850. (q) Courtney, A. H.; Puffer, E. B.; Pontrello, J. K.; Yang, Z.-Q.; Kiessling, L. L. *Proc. Natl. Acad. Sci. U. S. A.* **2009**, *106*, 2500–2505. (r) El-Boubbou, K.; Gruden, C.; Huang, X. *J. Am. Chem. Soc.* **2002**, *129*, 13392–13393. (s) Charych, D. H.; Nagy, J. O.; Spevak, W.; Bednarski, M. D. *Science* **1993**, *261*, 585–588.
- (15) (a) Adak, A. K.; Li, B. Y.; Lin, C. C. *Carbohydr. Res.* **2015**, *405*, 2–12. (b) Reichardt, N. C.; Martin-Lomasab, M.; Penades, S. *Chem. Soc. Rev.* **2013**, *42*, 4358–4376.
- (16) (a) de la Fuente, J. M.; Eaton, P.; Barrientos, A. G.; Rojas, T. C.; Rojo, J.; Canada, J.; Fernandez, A.; Penades, S. *Angew. Chem., Int. Ed.* **2001**, *40*, 2257–2261. (b) Otsuka, H.; Akiyama, Y.; Nagasaki, Y.; Kataoka, K. *J. Am. Chem. Soc.* **2001**, *123*, 8226–8230. (c) Lin, C.-C.; Yeh, Y.-C.; Yang, C.-Y.; Chen, C.-L.; Chen, G.-F.; Chen, C.-C.; Wu, Y.-C. *J. Am. Chem. Soc.* **2002**, *124*, 3508–3509. (d) Parry, A. L.; Clemson, N. A.; Ellis, J.; Bernhard, S. S. R.; Davis, B. G.; Cameron, N. R. *J. Am. Chem. Soc.* **2013**, *135*, 9362–9365.
- (17) (a) Robinson, A.; Fang, J.-M.; Chou, P.-T.; Liao, K.-W.; Chu, R.-M.; Lee, S.-J. *ChemBioChem* **2005**, *6*, 1899–1905. (b) Ohyanagi, T.; Nagahori, N.; Shimawaki, K.; Hinou, H.; Yamashita, T.; Sasaki, A.; Jin, T.; Iwanaga, T.; Kinjo, M.; Nishimura, S.-I. *J. Am. Chem. Soc.* **2011**, *133*, 12507–12517. (c) Kikkeri, R.; Lepenies, B.; Adibekian, A.; Laurino, P.; Seeberger, P. H. *J. Am. Chem. Soc.* **2009**, *131*, 2110–2112. (d) Chen, C.-T.; Munot, Y. S.; Salunke, S. B.; Wang, Y.-C.; Lin, R.-K.; Lin, C.-C.; Chen, C.-C.; Liu, Y.-H. *Adv. Funct. Mater.* **2008**, *18*, 527–540. (e) Xie, M.; Liu, H. H.; Chen, P.; Zhang, Z. L.; Wang, X. H.; Xie, Z. X.; Du, Y.; Pan, B. Q.; Pang, D. W. *Chem. Commun.* **2005**, 5518–5520. (f) Babu, P.; Sinha, S.; Surolia, A. *Bioconjugate Chem.* **2007**, *18*, 146–151.
- (18) (a) van Kasteren, S. I.; Campbell, S. J.; Serres, S.; Anthony, D. C.; Sibson, N.; Davis, B. G. *Proc. Natl. Acad. Sci. U. S. A.* **2009**, *106*, 18–23. (b) Farr, T. D.; Lai, C.-H.; Grunstein, D.; Orts-Gil, G.; Wang, C.-C.; Boehm-Sturm, P.; Seeberger, P. H.; Harms, C. *Nano Lett.* **2014**, *14*, 2130–2134. (c) El-Boubbou, K.; Zhu, D. C.; Vasileiou, C.; Borhan, B.; Prosperi, D.; Li, W.; Huang, X. *J. Am. Chem. Soc.* **2010**, *132*, 4490–4499. (d) Gao, J.; Gu, H.; Xu, B. *Acc. Chem. Res.* **2009**, *42*, 1097–1107.
- (19) Lai, C.-H.; Lin, C.-Y.; Wu, H.-T.; Chan, H.-S.; Chuang, Y.-J.; Chen, C.-T.; Lin, C.-C. *Adv. Funct. Mater.* **2010**, *20*, 3948–3958.
- (20) Eklind, K.; Gustafsson, R.; Tidén, A. K.; Norberg, T.; Åberg, P. *M. J. Carbohydr. Chem.* **1996**, *15*, 1161–1178.
- (21) (a) Park, K.; Tae, S. J.; Choi, B.; Kim, Y. S.; Moon, C.; Kim, S. H.; Lee, H. S.; Kim, J.; Kim, J.; Park, J.; Lee, J. H.; Lee, J. E.; Joh, J. W.; Kim, S. *Nanomedicine* **2010**, *6*, 263–276. (b) Hwang, D. W.; Ko, H. Y.; Kim, S.-K.; Kim, D.; Lee, D. S.; Kim, S. *Chem.—Eur. J.* **2009**, *15*, 9387–9393. (c) Kim, T. H.; Kim, J. K.; Shim, W.; Kim, S. Y.; Park, T. J.; Jung, J. Y. *Magn. Reson. Imaging* **2010**, *28*, 1004–1013.
- (22) Park, S.; Lee, M. -R.; Shin, I. *Bioconjugate Chem.* **2009**, *20*, 155–162.
- (23) Fujimoto, S.; Ojo, O. O.; Arnqvist, A.; Wu, J. Y.; Odenbreit, S.; Haas, R.; Gaham, D. Y.; Yamaoka, Y. *Clin. Gastroenterol. Hepatol.* **2007**, *5*, 49–58.
- (24) Walz, A.; Odenbreit, S.; Mahdavi, J.; Borén, T.; Ruhl, S. *Glycobiology* **2005**, *15*, 700–708.
- (25) Messing, J.; Niehues, M.; Shevtsova, A.; Borén, T.; Hensel, A. *Molecules* **2014**, *19*, 3696–3717.
- (26) Tateno, H.; Mori, A.; Uchiyama, N.; Yabe, R.; Iwaki, J.; Shikanai, T.; Angata, T.; Narimatsu, H.; Hirabayashi, J. *Glycobiology* **2008**, *18*, 789–798.
- (27) (a) Bale, S. S.; Kwon, S. J.; Shah, D. A.; Banerjee, A.; Dordick, J. S.; Kane, R. S. *ACS Nano* **2010**, *4*, 1493–1500. (b) Gao, H.; Yang, Z.; Zhang, S.; Cao, S.; Shen, S.; Pang, Z.; Jiang, X. *Sci. Rep.* **2013**, *3*, 1–8.
- (c) Dombu, C. Y.; Kroubi, M.; Zibouche, R.; Matran, R.; Betbeder, D. *Nanotechnology* **2010**, *21*, 1–8.
- (28) (a) Choi, H.-J.; Choi, W.-S.; Park, J.-Y.; Kang, K.-H.; Prabagar, M. G.; Shin, C.-Y.; Kang, Y.-S. *Biomol. Ther.* **2010**, *18*, 271–279. (b) Rizzetto, L.; Kuka, M.; Filippo, C. D.; Cambi, A.; Netea, M. G.; Beltrame, L.; Napolitani, G.; Torcia, M. G.; D’Oro, U.; Cavalieri, D. *J. Immunol.* **2010**, *184*, 4258–4268.
- (29) Chang, M. C.; Pralle, A.; Isacoff, E. Y.; Chang, C. J. *J. Am. Chem. Soc.* **2004**, *126*, 15392–15393.